9-1-2008

Flame-retarded Polystyrene: Investigating Chemical Interactions between Ammonium Polyphosphate and MgAl Layered Double Hydroxide

Calistor Nyambo
Marquette University

Everson Kandare
University of Bolton

Dongyan Wang
Cornell University

Charles A. Wilkie
Marquette University, charles.wilkie@marquette.edu

Accepted version. *Polymer Degradation and Stability* , Vol. 93, No. 9 (September 2008): 1656-1663. DOI.

Polymer Degradation and Stability, Vol. 93, No. 9 (September 2008): 1656-1663. DOI.

Flame-Retarded Polystyrene: Investigating Chemical Interactions Between Ammonium Polyphosphate and MgAl Layered Double Hydroxide

Calistor Nyambo
Department of Chemistry and Center for Fire Retardant Research, Marquette University, Milwaukee, WI
Everson Kandare
Centre for Materials Research and Innovation, University of Bolton, BL3 5AB, UK
Dongyan Wang
Department of Materials Science and Engineering, Cornell University, 416 Bard Hall, Ithaca, NY
Charles A. Wilkie
Department of Chemistry and Center for Fire Retardant Research, Marquette University, Milwaukee, WI

Abstract

Potential flame retardants, MgAl-LDH and ammonium polyphosphate (APP), were added to neat polystyrene (PS) individually or in combinations at weight fractions no greater than 10%. Structural morphologies of MgAl-LDH and the corresponding PS nanocomposites were established via

X-ray diffraction (XRD) and transmission electron microscopy (TEM). Thermogravimetric analysis (TGA) and cone calorimetry were used to study the thermal stability and fire performance of the composites. Time to ignition is greatly reduced for PS composites when compared to the virgin polymer. Synergistic effects were observed in both TGA and cone calorimetry for formulations containing both MgAl-LDH and APP. Physical and chemical interactions between MgAl-LDH and APP are responsible for the observed synergy in thermal stability and fire performance.

Keywords

Polystyrene, Ammonium polyphosphate, Layered double hydroxide, Synergy

1. Introduction

Superior mechanical strength, gas barrier, optical, and flame retardant properties exhibited by polymer/layered inorganic nanocomposites (PLNs) will continue to fuel interest in this area of research [1], [2], [3], [4], [5], [6], [7]. The use of nanodimensional layered inorganic/organic hybrids as flame retardants (FRs) in thermoplastics has been studied and is fairly well understood, but their use in combination with conventional FR additives, such as ammonium polyphosphate (APP), is limited and very recent. The concept of using layered metal hydroxides together with phosphorus-containing flame retardant additives could be useful in improving the dispersion of these additives within the polymer matrix. Envisaged synergistic chemical interactions may also allow reductions in the overall additive concentration required to obtain satisfactory flame retardancy.

Layered double hydroxides (LDHs) are a subgroup of two-dimensional nanostructured materials commonly termed “hydrotalcite-like” in reference to their isomorphism with the natural occurring mineral hydrotalcite, $(Mg_6Al_2(OH)_{16})\ (CO_3)\cdot 4H_2O$. LDHs have the generic formula $\left[M^{2+}_{1-x}M^{3+}_{x}\cdot (OH)_2\right]^{x+}A^{n-}_{x/n}\cdot zH_2O$, consisting of positively charged metal hydroxide layers containing divalent and trivalent metal ions and inorganic or organic anions, A^{n-}, which serve to balance the charge as well as control the interlayer spacing. The great number of possible metal ion compositions and the ability to exchange intercalated anions are key factors in optimizing these materials for applications in fire retardancy. Intercalation of the desired anions is generally achieved via four approaches: (i) co-precipitation which requires addition of a solution containing M^{2+} and M^{3+} ions to an alkaline medium containing the desired intercalate, (ii) direct anionic exchange in a solution containing the desired anions under suitable conditions, (iii) re-hydration of calcined LDH precursor in a solution of desired anions, and (iv) thermal reactions [8].

In this work, an LDH based on Mg and Al has been chosen, since it resembles the commonly used fire retardant metal hydroxides, $Mg(OH)_2$ (MDH) and $Al(OH)_3\cdot 3H_2O$ (ATH), however, with the possibility of improving the dispersion through polymer intercalation and/or exfoliation. Pyrolysis products from the thermal decomposition of an MgAl-LDH are perceived to be generally non-toxic, rendering this additive suitable for addressing environmental concerns, which threaten the continued use of halogenated FRs. APP, a high molecular weight phosphate based chain, is of interest, since it serves as both an acid source and a blowing agent in intumescent formulations known to promote char formation during polymer decomposition. Phosphoric acids produced during pyrolysis promote charring while the evolved NH_3 improves swelling hence slowing or preventing heat and mass transfer to and from the pyrolysis zone.

We report herein the concomitant use of MgAl-LDH and APP in an attempt to develop FR formulations that will be effective with respect to multiple flame retardant requirements, however, at

low concentrations thus avoiding high loadings which might otherwise have detrimental effects on the mechanical properties.

2. Experimental

2.1. Materials

Polystyrene (M_w ca. 230 000, M_n ca. 140 000, melt index 6.0–9.0 g/10 min at 200 °C/5 kg), magnesium nitrate hexahydrate, (99%) [$Mg(NO_3)_2{\cdot}6H_2O$], aluminum nitrate nonahydrate, (99%) [$Al(NO_3)_3{\cdot}9H_2O$], sodium hydroxide, [NaOH], were obtained from Aldrich Chemical Co and 10-undecenoic acid, (98%) [$C_{11}H_{22}CO_2H$], referred herein as (U) was obtained from TCI. Magnesium aluminum carbonate LDH (Pural MG 61 HT) was kindly supplied by Sasol Germany GmbH. FTIR grade potassium bromide, [KBr], was supplied by Alfa Aesar. Ammonium polyphosphate was supplied by ICL Performance Products Inc. All chemicals were used as received without further purification.

2.2. Preparation of the layered double hydroxides

The layered double hydroxide MgAl-undecenoate (MAU-LDH) was prepared following a literature co-precipitation method [9]. A solution of $Mg(NO_3)_2{\cdot}6H_2O$ (20 mmol) and $Al(NO_3)_3{\cdot}9H_2O$ (10 mmol) in deionized and decarbonated water (50 mL) was added dropwise to a solution of undecenoic acid (20 mmol) and NaOH (20 mmol) in deionized and decarbonated water (100 mL) with vigorous mixing under an inert (N_2) atmosphere. The pH of the solution was maintained at 10.0 by adding 1 M NaOH solution. The resultant slurry was aged at 60 °C for 24 h, cooled to room temperature and repeatedly washed with deionized and decarbonated water before drying under an inert atmosphere at room temperature. Magnesium aluminum nitrate LDH was prepared following a procedure similar to that reported by Meyn et al. [10].

2.3. Preparation of the polystyrene composites

Polystyrene-LDH/APP composites were prepared via melt blending using established methods [11]. Polystyrene composites with *x*% MAU and *y*% APP (PS - MAU/APP - *x*/*y*) were prepared by melt blending on a Brabender mixer (temperature = 190 °C, screw speed = 60 rpm, and time = 10 min). Constitutive proportions of MAU-LDH and APP in composites samples are presented in Table 1. A reference sample of unmodified polystyrene was obtained by following the same procedure only without any additive.

Table 1. Composition of polystyrene composites

Sample	Polystyrene (%)	MAU-LDH (%)	APP (%)
PS	100	0	0
PS - MAU/APP - 0/5	95	0	5
PS - MAU/APP - 2.5/2.5	95	2.5	2.5
PS - MAU/APP - 5/0	95	5	0
PS - MAU/APP - 0/10	90	0	10
PS - MAU/APP - 5/5	90	5	5
PS - MAU/APP - 10/0	90	10	0

2.4. Instrumentation

Powder X-ray diffraction measurements (PXRD) were performed in a Bruker–Nonius APEX2, with a CCD detector with a 0.5 mm Monocap collimator and graphite monochromator with Cu (K

alpha) source λ = 1.54078 Å, from a sealed X-ray tube. The powder sample was prepared as a 0.3 mm ball using small amounts of mineral oil and was put on top of a 0.1 mm nylon pin. Data were collected at various 2ϑ values in 9° increments using 180° phi rotations. Basal spacing, d, of MAU-LDH and polystyrene nanocomposites were obtained from averaging 00*l* reflections after fitting the raw spectra to a pseudo-Voight function with XFIT [12] stripping off the Cu $K\alpha_2$ contributions.

Bright field transmission electron microscopy (TEM) images of the nanocomposites were obtained at 60 kV with a Zeiss 10C electron microscope. The samples were ultramicrotomed with a diamond knife on a Reichert–Jung Ultra-Cut E microtome at room temperature to give an ≈700 Å thick section. The sections were then transferred from the knife-edge to 600 hexagonal mesh Cu grids.

Fourier transform infrared spectra of undecenoic acid, MgAl–NO_3-LDH, MgAl–CO_3-LDH, and MAU-LDH were obtained using the KBr method on a Nicolet Magna-IR 560 spectrometer operated at 1 cm^{-1}resolution in the 400–4000 cm^{-1} region. Thermogravimetric analysis (TGA) and differential thermal analysis (DTA) were performed on a SDT 2960 simultaneous DTA–TGA instrument from 50 to 600 °C at a heating rate of 20 °C min^{-1} in N_2, flowing at 85 ± 5 mL min^{-1}, with sample sizes of 15.0 ± 1.0 mg contained in aluminum sample cups. Approximately 30 g of polystyrene composite samples were compression molded into 10 cm × 10 cm square plaques of uniform thickness (≈3 mm) before cone calorimetry was performed on an Atlas Cone 2 instrument at an incident flux of 35 kW m^{-2} with a cone shaped heater; the spark was continuous until the sample ignited. All samples were run in triplicate and the average value, with the standard deviation, is reported; results from the cone calorimeter are generally considered to be reproducible to ±10% [13].

3. Results and discussion

3.1. Characterization of MgAl-LDH and its PS composites

3.1.1. Infrared and X-ray diffraction analysis

An MgAl-LDH intercalated by undecenoate (U) was synthesized via co-precipitation from aqueous solutions. The presence of charge balancing undecenoate anions within the nanodimensional galleries was confirmed by the use of infrared spectroscopy (IR). The strong asymmetric and symmetric carboxylate stretching bands at 1560 and 1456 cm^{-1}, respectively, indicate that the carboxylic acid anion is incorporated into the LDH, Fig. 1[8]. The C $=$ C stretching vibration of 10-undecenoate anion occurs at 1639 cm^{-1} while its sp^2 C–H stretching vibration occurs at 3090 cm^{-1}. These FTIR assignments demonstrate that the 10-undecenoate anion is successfully intercalated into the LDH galleries. Furthermore the presence of undissociated undecenoic acid would have been identified by a strong carbonyl stretch at 1724 cm^{-1}. In addition, IR is useful to confirm the absence of impurity anions such as nitrate (1385 cm^{-1}) or carbonate (1365 cm^{-1}; asymmetric stretching vibrations), Fig. 1.

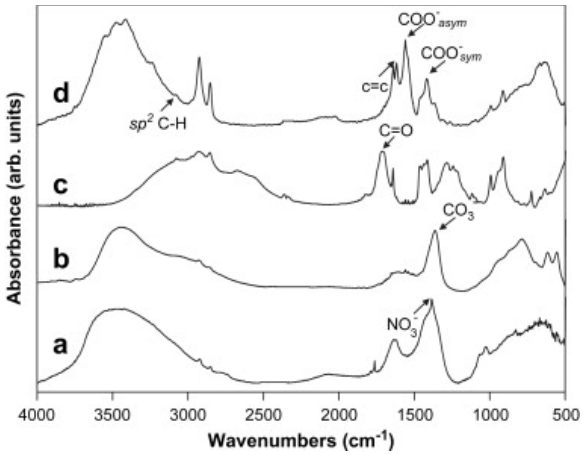

Fig. 1. FTIR spectra of (a) magnesium aluminum nitrate LDH, (b) magnesium aluminum carbonate LDH (Pural MG 61 HT), (c) undecenoic acid, and (d) MgAl-LDH. Spectra are offset for clarity.

The PXRD pattern for MAU-LDH is shown in Fig. 2. MAU-LDH exhibits strong, sharp, and symmetrical 00*l* basal reflections indicative of a well-crystallized phase revealing the existence of coherent diffraction planes in the *c*-dimension. Indexing of the PXRD patterns is based on a rhombohedral symmetry (prototype $3R_1$). Three equidistantly spaced basal reflections at 2ϑ positions of 3.9, 7.9, and 11.9° were observed corresponding to an average basal spacing, *d*, of 23.3 Å.

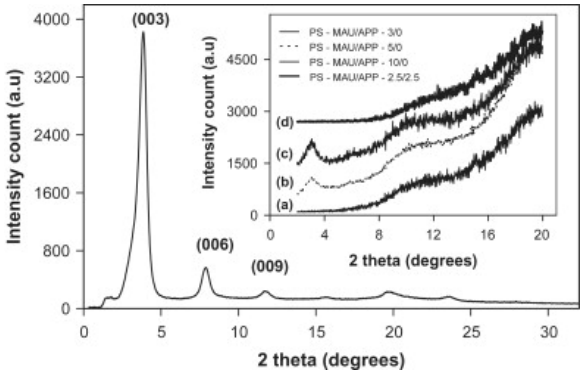

Fig. 2. Powder XRD pattern of MgAl-LDH. Insert: XRD patterns of PS composites (a) PS - MAU/APP - 3/0, (b) PS - MAU/APP - 5/0, (c) PS - MAU/APP - 10/0, and (d) PS - MAU/APP - 2.5/2.5 respectively. Data for the PS composites are offset for clarity but not otherwise scaled.

The chain length of undecenoate was determined to be 14.3 Å using a restricted Hartree–Fock (RHF) 6-31G level in Spartan [14]. Given that the thickness of the brucite-like layer has been reported to be 4.8 Å, subtracting this from 23.3 Å gives an interlayer space of 18.5 Å. Therefore, the observed basal spacing is consistent with a monolayer anionic arrangement within the galleries as reported by Wang and co-workers [9]. An XRD pattern for a formulation containing 3% MAU-LDH is shown as trace (a) in the insert of Fig. 2. Addition of MAU-LDH at such a low concentration may lead to an exfoliated polymer nanocomposite as suggested by the absence of basal reflections in the XRD pattern at low 2ϑvalues. However, XRD 001 reflections for polystyrene formulations containing 5% and 10% MAU-LDH are shifted to a lower 2ϑ value of 3.1°. The basal spacings for PS - MAU/APP - 5/0 and PS - MAU/APP - 10/0 were calculated to be 28.7 Å indicating the infusion of polystyrene chains into the galleries, consequently enlarging the interlayer space between the LDH layers. As the concentration of the additives is increased it becomes consistently harder to obtain a homogeneous dispersion of clay platelets at the nanometer level. When 2.5% of MAU-LDH is concomitantly added with 2.5% APP no basal reflections are observed at low 2ϑ values suggesting a substantial degree of exfoliation.

3.1.2. Transmission electron microscopy

While XRD analysis is useful in evaluating the morphology of polymer/inorganic hybrid composites, it alone does not provide all the information required. Thus, transmission electron microscopy (TEM) provides a complimentary means of directly assessing the existence of intercalated or exfoliated phases of layered inorganic materials within the polymer matrix. Low magnification images provide information about the degree of dispersion at the nanoscale or microscale levels while high magnification images give information about the particular morphology, exfoliation and/or intercalation, that has been achieved.

The TEM images of PS containing 3% MAU-LDH at low and high magnifications are shown in Fig. 3(a and b) respectively. The TEM image at low magnification, Fig. 3(a), suggests very good dispersion of the layered nanoclay at the nanoscale level, while the high magnification image suggests exfoliation consistent with the XRD results shown in Fig. 2. Poor dispersion of the LDH is observed on increasing the loading of MAU-LDH from 3% to 5%, Fig. 3(c). In some areas on the microscopic image, aggregates with an average diameter of 0.5 µm are observed, suggesting the formation of a microcomposite. These observations are consistent with the presence of intercalated polymer phases observed via XRD. This assertion is confirmed at higher magnification as evident from the presence of clearly visible tactoids, Fig. 3(d).

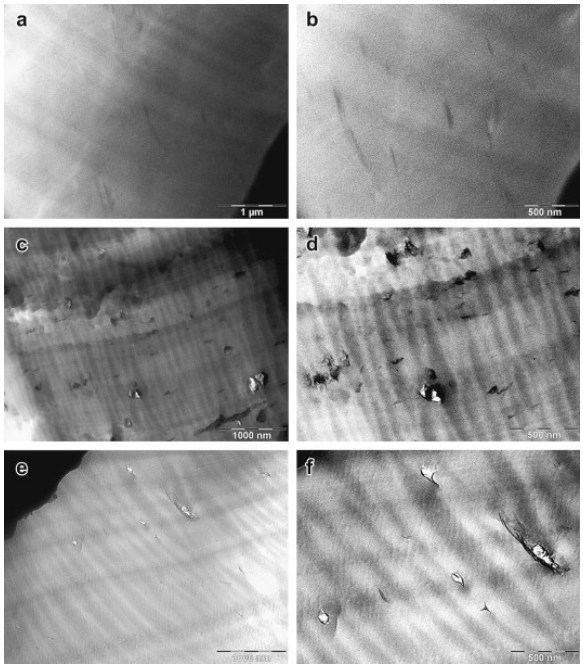

Fig. 3. TEM images at (a) low and (b) high magnification for PS - MAU/APP - 3/0, (c) low and (d) high magnification for PS - MAU/APP - 5/0, and (e) low and (f) high magnification for PS - MAU/APP - 2.5/2.5. The scale bars for low and high magnification represent 500 nm and 1000 nm distances respectively.

Comparison between PS - MAU/APP - 5/0 and a formulation in which some of the MAU-LDHs is replaced with APP, PS - MAU/APP - 2.5/2.5, reveals an improvement in the overall additive dispersion as seen from the presence of a smaller number of tactoids in the low magnification TEM image, Fig. 3(e). Tactoids with an average length of 0.5 µm are observed in the high magnification image, Fig. 3(f). However, these tactoids may be due to the agglomeration of APP alone and not necessarily from the poor dispersion of the LDH; otherwise the XRD pattern, Fig. 2 insert trace (d), would have revealed the presence of an intercalated phase. While the concomitant presence of MAU-

LDH and APP is efficient in improving some of the flammability properties and thermal stability of PS, the resultant compromised dispersion of the additives may have a detrimental effect on the mechanical properties of the polymer composites.

3.2. Thermal stability of MgAl-LDH, APP and their PS composites

The thermal characteristics of LDHs containing different metal ions and charge balancing anions result in tailoring these inorganic/organic hybrids for many potential applications such as stationary phases in gas chromatography [15], catalysis and fire retardancy [16]. The thermal decomposition of layered inorganic/organic hybrids is generally divided into three stages: (i) dehydration of physiosorbed and intercalated water, (ii) dehydroxylation and (iii) deanation followed by oxidative degradation of organic anions. Previously, in work from these laboratories, the thermal decomposition of hydroxy double salts (HDSs), structurally similar to LDHs, was investigated and the above mentioned stages were confirmed [17]. Redox chemical reactions involving the transition metals are expected and these are anticipated to prevent or slow the depolymerization process when the LDH is combined with polystyrene.

At elevated temperatures, the phosphorus containing the flame retardant additive, APP, decomposes to produce phosphoric and polyphosphoric acids, which consequently promote charring via cross-linking of reactive polymer fragments [18]. The formation of carbonized char networks prevents or slows the transfer of heat, oxygen and combustible volatiles into the pyrolysis zone; hence retarding the flaming/combustion process. Detailed mechanistic schemes describing the charring behavior of APP containing resin formulations have been discussed by Kandola and co-workers [19].

The TGA curves for the unmodified polystyrene and its composites are shown in Fig. 4, Fig. 5, where degradation occurs in a single step (300–500 °C) via statistical β-scission of the polystyrene chains with the evolution of styrene and its oligomers, α-methyl styrene, benzene, toluene and CO_2 as major gaseous products leaving negligible residual char [20], [21]. The onset of thermal degradation for the unmodified polystyrene, measured as the temperature at which 10% mass loss occurs, T_{10}, is 399 °C while T_{max}, the temperature at which the maximum mass loss occurs is 431 °C. T_{10} is shifted to lower temperatures when APP is used alone but to higher values when MAU-LDH is used alone or in combination with APP. Significant T_{10} delays observed for formulations containing both APP and MAU-LDH at cumulative concentrations of 5% and 10% suggest synergistic interactions in the thermal stabilization of PS. The maximum decomposition stage for modified PS composites occurs at temperatures lower than that observed for the neat polymer. Detailed information about onset, maximum decomposition temperatures, and residual char yields is given in Table 2.

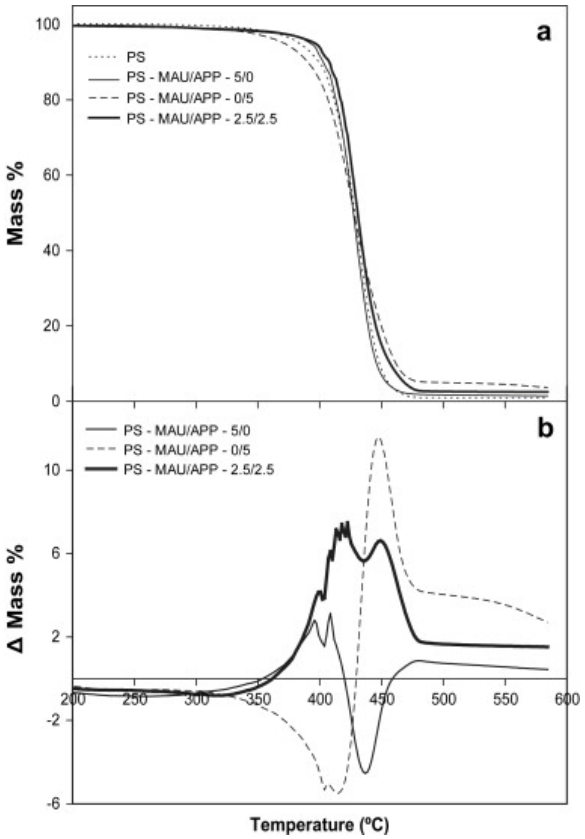

Fig. 4. (a) TGA curves for neat PS (dotted), PS - MAU/APP - 5/0 (solid), PS - MAU/APP - 0/5 (dashed) and PS - MAU/APP - 2.5/2.5 (bold). (b) Curves of mass loss differences as a function of degradation temperature for PS composites at 5% loadings for PS - MAU/APP - 5/0 (solid), PS - MAU/APP - 0/5 (dashed) and PS - MAU/APP - 2.5/2.5 (bold).

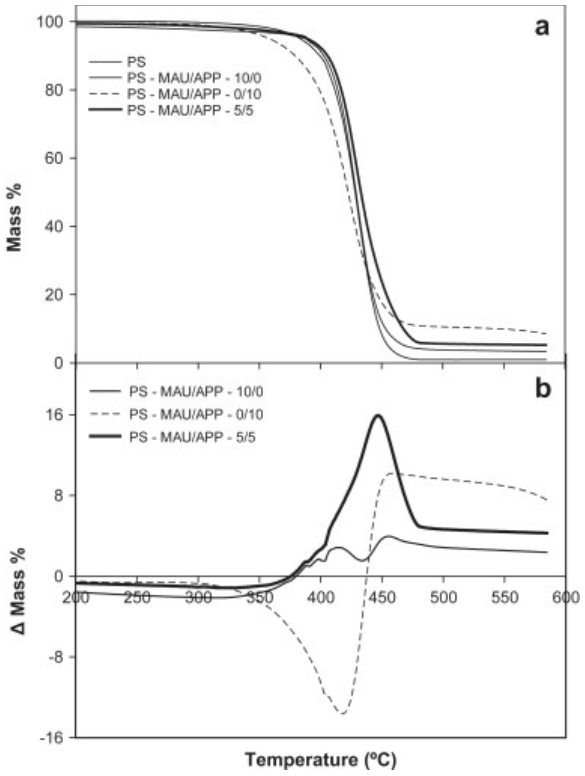

Fig. 5. (a) TGA curves for neat PS (dotted), PS - MAU/APP - 10/0 (solid), PS - MAU/APP - 0/10 (dashed) and PS - MAU/APP - 5/5 (bold). (b) Curves of mass loss differences as a function of degradation temperature for PS composites at 5% loadings for PS - MAU/APP - 10/0 (solid), PS - MAU/APP - 0/10 (dashed) and PS - MAU/APP - 5/5 (bold).

Table 2. TGA data for polystyrene and its composites

Sample	**Temperature (°C)**				**Char (%)**
	T_{onset}	ΔT_{onset}	T_{max}	ΔT_{max}	
PS	399	–	431	–	1
PS - MAU/APP - 0/5	390	−9	424	−7	4
PS - MAU/APP - 2.5/2.5	408	9	430	−1	3
PS - MAU/APP - 5/0	403	4	429	−2	1
PS - MAU/APP - 0/10	379	−20	422	−9	10
PS - MAU/APP - 5/5	405	6	429	−2	5
PS - MAU/APP - 10/0	402	3	430	−1	3

T_{10}, Temperature at which 10% mass loss occurs; T_{max}, temperature at which maximum mass loss occurs; ΔT_{max}, T_{max} (composites) minus T_{max} (neat PS).

Mass difference curves, Δ mass % (mass % of PS composites minus mass % of unmodified PS at the same temperature) for polystyrene composites are shown in Fig. 4, Fig. 5. Positive Δ mass % values at any given temperature mean that the PS composites are thermally more stable than the virgin polymer while negative values indicate, the reverse, lower thermal stability. The Δ mass % curve of an MAU containing PS nanocomposites, PS - MAU/APP - 5/0, is negative at temperatures below 350 °C and between 430 and 460 °C but positive between 350 and 430 °C and at temperatures greater than 460 °C. Increasing the weight percent of MAU to 10%, Fig. 5(b), destabilizes PS at temperatures below 380 °C but improves its thermal stability at temperatures above 380 °C.

Addition of APP at 5% greatly compromises the thermal stability of PS below 430 °C while promoting char formation at temperatures above 430 °C. A similar effect is observed when the weight percent of APP is increased to 10%, Fig. 5(b). The combination of MAU and APP, as in PS - MAU/APP - 2.5/2.5 and PS - MAU/APP - 5/5, results in positive Δ mass % for temperatures above 370 °C. Maximum stabilization (430–450 °C) occurs within a temperature range over which the maximum mass loss rate is observed for PS. Addition of MAU together with APP therefore serves to prevent or slow depolymerization occurring via random chain scission, perhaps through synergistic interactions.

The overall stabilization effect (OSE) of MAU and APP individually or combined at specified percent loadings is calculated via integration of the area under the Δ mass % versus temperature curve using the following equation:

$$\mathrm{OSE} = \sum_{T=50}^{600}((\mathrm{mass\%flameretardedPSsample}_T) - (\mathrm{mass\%unmodifiedPS}_T)) \quad (1)$$

where T is the temperature of degradation (T = 50–600 °C) and the results are presented in Fig. 6. A negative OSE value, −34%, is observed for 5% MAU suggesting that at this level the additive has an overall destabilization effect. The OSE values are positive for the rest of the formulations. However, the combination of APP and MAU significantly improves the thermal stability of PS as measured by OSE values relative to when they are used individually. The calculated OSE value for a formulation with 5% MAU and 5% APP (PS - MAU/APP - 5/5) is 635% while the OSE values obtained for MAU and APP when

used individually at 10% loading are 75% and 265% respectively. These results suggest synergistic interactions; the combined stabilization effect is higher than a mere additive effect.

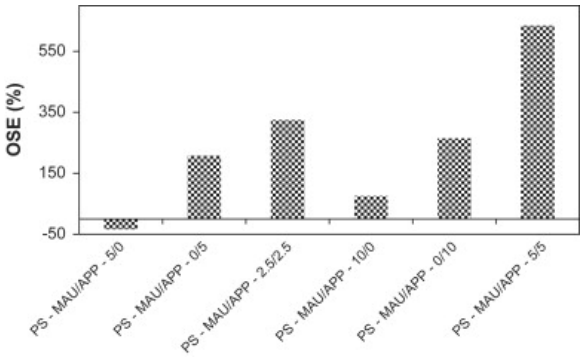

Fig. 6. Overall stabilization effect (OSE) of flame retardant-containing formulations.

The combination of APP and MAU-LDH in polystyrene is anticipated to be chemically interactive, thus promoting the formation of "char bonded structures". In order to evaluate synergistic and/or antagonistic interactions between APP and MAU-LDH, theoretical mass loss profiles were calculated from a linear combination of their TGA profiles for the individual components and compared to the experimental data. Fig. 7 shows the TGA mass loss profile of a 1:1 mixture of PS - MAU/APP - 5/0 and PS - MAU/APP - 0/5 calculated from the linear combination of their individual profiles and the experimentally obtained mass loss profile of PS - MAU/APP - 2.5/2.5. Shown also is the mass difference between the experimental and calculated data. Analysis of these data suggests enhanced char formation when APP is used together with the LDH as compared to when they are used individually.

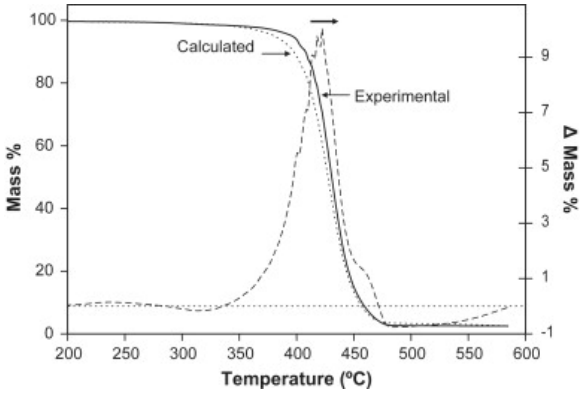

Fig. 7. Calculated TG mass loss versus temperature for a 1:1 mixture of PS - MAU/APP - 5/0 and PS - MAU/APP - 0/5 calculated from a linear combination of their individual profiles and also the experimentally obtained mass loss profile of PS - MAU/APP - 2.5/2.5.

The exact mechanism of interaction between APP and the LDH when interspersed in polystyrene resin is not known; however, it is anticipated that these additives slow or prevent depolymerization of the polystyrene chains. Probably, water from de-intercalation and dehydroxylation processes catalyze the formation of polyphosphoric acids which, in turn, promotes the formation of a char network leading to the retardation of the thermo-oxidative degradation rate.

3.3. Flammability behavior of PS composites

The flammability behavior of flame retardant PS composites has been evaluated by cone calorimetry. The effect of adding the potential fire retardant additives, MAU and APP, to PS individually or together has been investigated. The data obtained from cone calorimetry include the time to

sustained ignition, t_{ign}; the heat release rate, and especially the peak value (PHRR); the total heat release (THR); the average mass loss rate (AMLR); and the average specific extinction area (ASEA), a measure of the amount of smoke produced during combustion. Cone calorimetry can also provide useful information on nanocomposites formation with montmorillonite (MMT) since MMT microcomposites give effectively no reduction in PHRR and AMLR while polymer-MMT nanocomposites give considerable reductions [22], [23]. The applicability of this to LDH-containing systems has not been shown.

The heat release rate and mass loss rate curves for the unmodified PS and its flame-retarded composites are shown in Fig. 8, Fig. 9 and the data presented in Table 3. The time to sustained ignition, t_{ign}, is significantly reduced upon addition of APP and MAU individually or in combination. The addition of these fire retardants to PS is expected to increase the viscosity of the neat polymer reducing heat exchange between the sample surface exposed to the radiant source and the bulk of the sample. This would result in a rapid increase in the surface temperature of the sample; hence the time required for the sample to reach the pyrolysis temperature is significantly reduced [24].

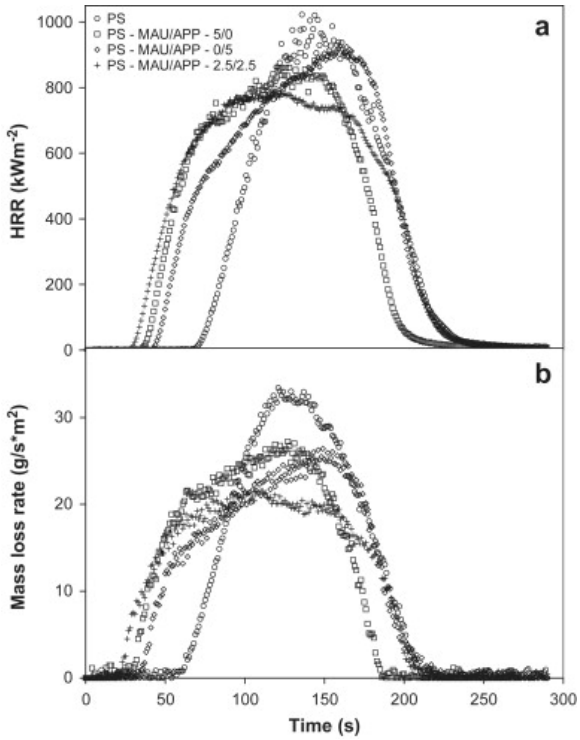

Fig. 8. (a) Heat release rate curves for neat PS (circles), PS - MAU/APP - 5/0 (squares), PS - MAU/APP - 0/5 (diamonds) and PS - MAU/APP - 2.5/2.5 (crosses) from cone calorimetry measurements at 35 kW m^{-2}. (b) Mass loss rate curves for neat PS (circles), PS - MAU/APP - 5/0 (squares), PS - MAU/APP - 0/5 (diamonds) and PS - MAU/APP - 2.5/2.5 (crosses) from cone calorimetry measurements at 35 kW m^{-2}.

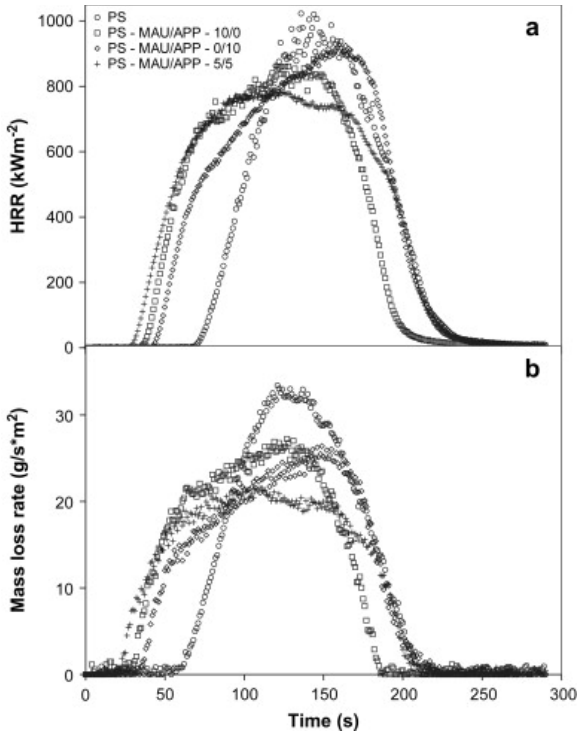

Fig. 9. (a) Heat release rate curves for neat PS (circles), PS - MAU/APP - 10/0 (squares), PS - MAU/APP - 0/10 (diamonds) and PS - MAU/APP - 5/5 (crosses) from cone calorimetry measurements at 35 kW m^{-2}. (b) Mass loss rate curves for neat PS (circles), PS - MAU/APP - 10/0 (squares), PS - MAU/APP - 0/10 (diamonds) and PS - MAU/APP - 5/5 (crosses) from cone calorimetry measurements at 35 kW m^{-2}.

Table 3. Cone calorimetry data for PS composites at 35 kW m^{-2}

Sample	**t_{ign} (s)**	**PHRR (kW m^{-2}) (% red)**	**t_{PHRR} (s)**	**THR (MJ m^{-2})**	**AMLR (g sm^{-2})**	**CY (%)**
PS	63 ± 4	1111 ± 33	141 ± 5	98 ± 1	28 ± 1	0
PS - MAU/APP - 0/5	39 ± 1	986 ± 59 (11)	160 ± 2	104 ± 4	23 ± 1	6 ± 1
PS - MAU/APP - 2.5/2.5	25 ± 1	808 ± 26 (27)	129 ± 30	107 ± 3	20 ± 1	8 ± 2
PS - MAU/APP - 5/0	35 ± 1	924 ± 30 (17)	139 ± 6	96 ± 2	25 ± 2	2 ± 0
PS - MAU/APP - 0/10	34 ± 5	862 ± 18 (22)	162 ± 4	98 ± 2	20 ± 1	8 ± 1
PS - MAU/APP - 5/5	25 ± 1	642 ± 17 (42)	108 ± 8	101 ± 1	16 ± 1	11 ± 2
PS - MAU/APP - 10/0	35 ± 5	815 ± 14 (27)	123 ± 14	95 ± 2	22 ± 1	4 ± 1

t_{ign}, Time to ignition; PHRR, peak heat release rate; (% red), reduction in PHRR; t_{PHRR}, time to peak heat release rate; THR, total heat release; AMLR, average mass loss rate; CY, char yield (%).

PS composites containing 5% and 10% MAU show reductions in PHRR of 17% and 27% respectively. When APP is added to PS at the same weight fractions lower PHRR reductions were observed, 11% and 22%, respectively. Even though MAU alone is more effective in reducing the PHRR than APP, it is envisaged that their combination will yield results better than simply an additive effect. The observed reduction in PHRR, 42%, for PS - MAU/APP - 5/5 is significantly higher than would have been obtained if the flame retardant effects of MAU and APP were additive, 28%, Fig. 10. Synergistic interactions between MAU and APP are thus implied in order to explain the observed results.

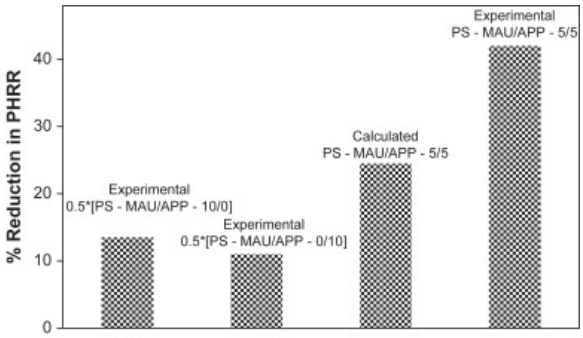

Fig. 10. Experimental and calculated additive % reduction in PHRR for PS - MAU/APP - 5/0, PS - MAU/APP - 0/5 and PS - MAU/APP - 5/5.

Water is one of the primary products released during the thermal decomposition of LDHs and is an essential ingredient in the formation of phosphoric and polyphosphoric acids which subsequently promote char formation. Thus the simultaneous presence of MAU, APP, and their decomposition products together with PS efficiently promotes formation of char, a physical barrier, and obviously participates in chemical reactions retarding depolymerization processes. The reduction in PHRR suggests formation of polystyrene nanocomposites, in agreement with XRD and TEM [22], [23].

Mass loss rates in Fig. 8, Fig. 9 mirror the heat release rates for the unmodified PS and its composites. Reductions in PHRR are a result of a reduction in the production of combustible volatile species. The presence of MAU and APP and their decomposition products during the thermal decomposition of PS slows chain scissions which would have led to the formation of volatiles, the fuel necessary to the flame. The total heat release, THR, values of PS composites presented in Table 3 are within experimental error of the neat polymer, suggesting that the polymer fraction within the composite does completely decompose at the conclusion of the experiment.

Char yields were determined from cone calorimetry data and are presented in Table 3. The unmodified PS sample gave no residual char, consistent with TGA results. However, flame-retarded PS formulations gave residual char amounts significantly above the expected levels at the conclusion of the experiments, suggesting that MAU and APP enhance the cross-linking of degradation by-products to form carbonaceous char. PS composites containing 5% and 10% MAU gave residual char amounting to 2% and 4% respectively. The residual char is possibly due to metal oxides remaining after complete combustion of the polystyrene which is otherwise suggested by no reduction in the observed THR values. When APP is added to PS at the same weight fractions more residual char was observed, 6% and 8%, respectively. It is anticipated that the combination of MAU with APP will promote char formation and yield improvements better than simply of an additive effect. The observed char yields, 8%, for PS - MAU/APP - 2.5/2.5 and, 11%, for PS - MAU/APP - 5/5 are significantly higher than would have been obtained if the promotion of char formation by MAU and APP was additive, 4% and 6%, respectively. Synergistic chemical interactions between MAU and APP are proposed in order to explain the observed phenomenon.

Photographs of residual char formed from the flame-retarded PS samples following cone calorimetry differ in appearance, depending upon the additives, and are presented in Fig. 11. The residual char from the formulation containing MAU alone, PS - MAU/APP - 10/0, was spongy and uniformly distributed while that from PS - MAU/APP - 0/10 was firm and intact and uniformly distributed. A very distinct difference in appearance was observed for the residual char from PS - MAU/APP - 5/5 which was intact but brittle and appeared as clusters. The morphology of the residual char dictates its efficiency in slowing the flaming process. A highly dense and impermeable char

network would prevent the diffusion of volatiles and oxygen to the pyrolysis zone, thus retarding the combustion process. This may explain why formulations containing MAU and APP showed better fire resistance as compared to the other formulations.

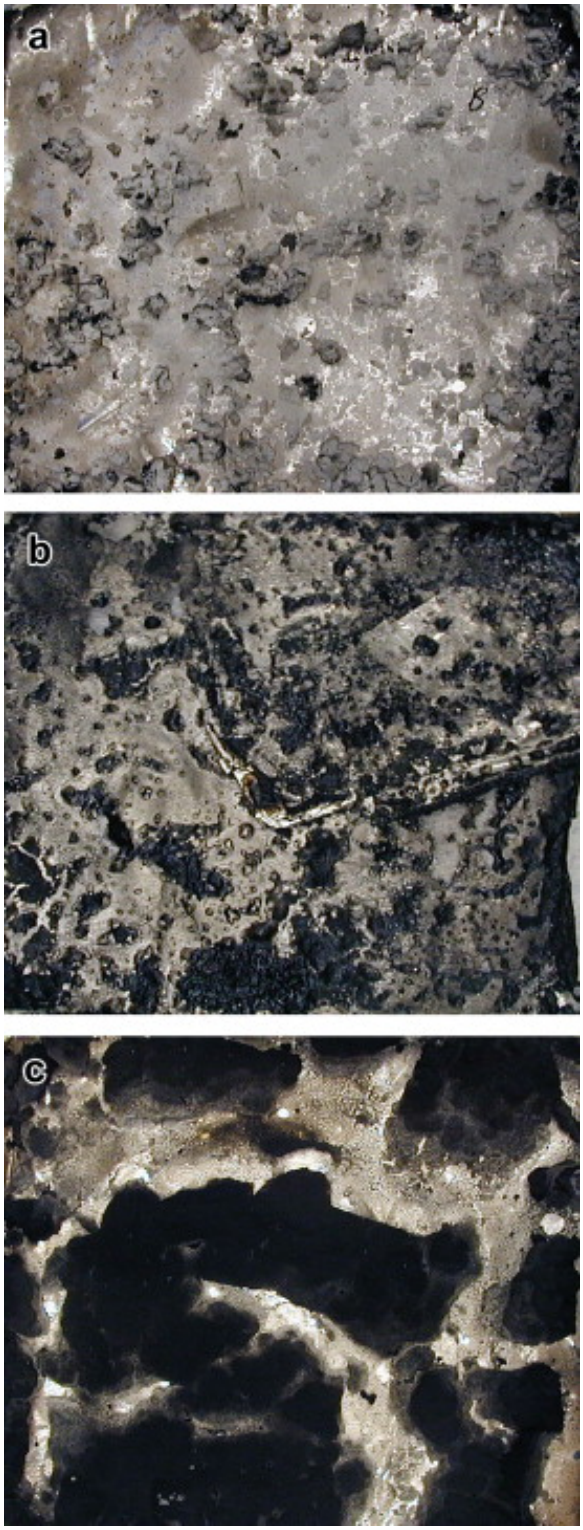

Fig. 11. Photographs of residual char from (a) PS - MAU/APP - 10/0, (b) PS - MAU/APP - 0/10, and (c) PS - MAU/APP - 5/5 formulations following cone calorimetry tests under a heat flux of 35 kW m^{-2}.

4. Conclusions

Polystyrene composites containing a layered inorganic/organic hybrid MAU-LDH and APP were prepared via melt blending and their morphology evaluated using XRD, TEM and cone calorimetry. Thermogravimetric analysis reveals that the presence of MAU and APP individually has small effects on the thermal stability and char formation. However, when added together, MAU and APP show a notable stabilization effect in the thermo-oxidative degradation stage while promoting the formation of char at high temperatures. Addition of MAU and APP at a weight percent no more than 10% results in significant reductions in the peak heat release rate (PHRR) as measured using cone calorimetry. Similar reductions are observed for the average mass loss rate (AMLR) suggesting that the reductions in PHRR are due to the slower rate at which combustible volatiles are produced.

Acknowledgements

The authors gratefully thank Dr Jeanne Hossenlopp for helpful discussions and Dr Sergey Lindeman for performing the powder X-ray diffraction analysis.

References

[1] M. Alexandre, P. Dubois. **Polymer-layered silicate nanocomposites: preparation, properties and uses of a new class of materials** *Mater Sci Eng*, R28 (2000), pp. 1-63

[2] P. Ding, B.J. Qu. **Synthesis and characterization of exfoliated polystyrene/ZnAl layered double hydroxide nanocomposite via emulsion polymerization.** *J Colloid Interface Sci*, 291 (2005), pp. 13-18

[3] L. Qiu, W. Chen, B. Qu. **Structural characterisation and thermal properties of exfoliated polystyrene/ZnAl layered double hydroxide nanocomposites prepared via solution intercalation.** *Polym Degrad Stab*, 87 (2005), pp. 433-440

[4] L. Vieille, E.M. Moujahid, C. Taviot-Guého, J. Cellier, J.-P. Besse, F. Leroux. **In situ polymerization of interleaved monomers: a comparative study between hydrotalcite and hydrocalumite host structures.** *J Phys Chem Solids*, 65 (2004), pp. 385-393

[5] F.R. Costa, B.K. Satapathy, U. Wagenknecht, R. Weidisch, G. Heinrich. **Morphology and fracture behaviour of polyethylene/Mg-Al layered double hydroxide (LDH) nanocomposites.** *Eur Polym J*, 42 (2006), pp. 2140-2152

[6] W. Chen, L. Feng, B. Qu. **In situ synthesis of poly(methyl methacrylate)/MgAl layered double hydroxide nanocomposite with high transparency and enhanced thermal properties.** *Solid State Commun*, 130 (2004), pp. 259-263

[7] G.-A. Wang, C.-C. Wang, C.-Y. Chen. **The disorderly exfoliated LDHs/PMMA nanocomposites synthesized by in situ bulk polymerization: the effects of LDH-U on thermal and mechanical properties.** *Polym Degrad Stab*, 91 (2006), pp. 2443-2450

[8] S.P. Newman, W. Jones. **Synthesis, characterization and applications of layered double hydroxides containing organic guests.** *New J Chem*, 22 (1998), pp. 105-115

[9] G.-A. Wang, C.-C. Wang, C.-Y. Chen. **The disorderly exfoliated LDHs/PMMA nanocomposite synthesized by in situ bulk polymerization.** *Polymer*, 46 (2005), pp. 5065-5074

[10] M. Meyn, K. Benecke, G. Lagally. **Anion exchange reactions of layered double hydroxides.** *Inorg Chem*, 29 (1990), pp. 5201-5207

[11] D. Wang, J. Zhu, Q. Yao, C.A. Wilkie. **A comparison of various methods for the preparation of polystyrene and poly(methyl methacrylate) clay nanocomposites.** *Chem Mater*, 14 (2002), pp. 3837-3843

[12] Cheary R.W.; Coelho A.A. Programs XFIT and FOURYA, deposited in CCP14. Powder Diffraction Library, Engineering and Physical Sciences Research Council, Daresbury Laboratory, Warrington, England. http://www.ccp14.ac.uk/tutorial/xfit-95/xfit.htm, 1996.

[13] J.W. Gilman, T. Kashiwagi, M. Nyden, J.E.T. Brown, C.L. Jackson, S. Lomakin, *et al.* S. Al-Maliaka, A. Golovoy, C.A. Wilkie (Eds.), *Chemistry and technology of polymer additives*, Blackwell Scientific, London (1999), pp. 249-265

[14] **PC Spartan 2.0.** Wavefunction Inc, Irvine, CA (1999)

[15] M. Jakupca, P.K. Dutta. **Thermal and spectroscopic analysis of a fatty acid-layered double-metal hydroxide and its application as a chromatographic stationary phase.** *Chem Mater*, 7 (1995), pp. 989-994

[16] P.B. Messersmith, S.I. Stupp. **High-temperature chemical and microstructural transformations of a nanocomposite organoceramic.** *Chem Mater*, 7 (1995), pp. 454-460

[17] E. Kandare, J.M. Hossenlopp. **Thermal degradation of acetate-intercalated hydroxy double and layered hydroxy salts.** *Inorg Chem*, 45 (2006), pp. 3766-3773

[18] B.K. Kandola, R.A. Horrocks, P. Myler, D. Blair. **New developments in flame retardancy of glass-reinforced epoxy composites.** *J Appl Polym Sci*, 88 (2003), pp. 2511-2521

[19] B.K. Kandola, S. Horrocks, R.A. Horrocks. **Evidence of interaction in flame-retardant fibre-intumescent combinations by thermal analytical techniques.** *Thermochim Acta*, 294 (1997), pp. 113-125

[20] Y. Hu, S. Li. **The effects of magnesium hydroxide on flash pyrolysis of polystyrene.** *J Anal Appl Pyrol*, 78 (2007), pp. 32-39

[21] N. Grassie, G. Scott. **Polymer degradation and stabilization.** Cambridge University Press (1985)

[22] J. Zhu, P. Start, K.A. Mauritz, C.A. Wilkie. **Thermal stability and flame retardancy of poly(methyl methacrylate)-clay nanocomposites.** *Polym Degrad Stab*, 77 (2002), pp. 253-258

[23] M. Zanetti, G. Camino, D. Canavese, A.B. Morgan, F.J. Lamelas, C.A. Wilkie. **Fire retardant halogen-antimony-clay synergism in polypropylene layered silicate nanocomposites.** *Chem Mater*, 14 (2002), pp. 189-193

[24] Nazaré S., Hull T.R., Biswas B. Study of relationship between rheological and flammability properties of flame retarded poly(butylene terephthalate) containing nanoclays. In: 18th annual BCC conference on flame retardancy of polymeric materials, 21–23 May 2007, Stamford, USA.